Verification and Proper Use of Water-Oil Transfer Function for Dual-Porosity and Dual-Permeability Reservoirs

A. Balogun, SPE, Shell E&P, **H. Kazemi,** SPE, **E. Ozkan,** SPE, **M. Al-Kobaisi,** SPE, and **B. Ramirez,** SPE, Colorado School of Mines

Summary

Accurate calculation of multiphase fluid transfer between the fracture and matrix in naturally fractured reservoirs is a very crucial issue. In this paper, we will present the viability of the use of a simple transfer function to accurately account for fluid exchange resulting from capillary and gravity forces between fracture and matrix in dual-porosity and dual-permeability numerical models. With this approach, fracture- and matrix-flow calculations can be decoupled and solved sequentially, improving the speed and ease of computation. In fact, the transfer-function equations can be used easily to calculate the expected oil recovery from a matrix block of any dimension without the use of a simulator or oil-recovery correlations.

The study was accomplished by conducting a 3-D fine-grid simulation of a typical matrix block and comparing the results with those obtained through the use of a single-node simple transfer function for a water-oil system. This study was similar to a previous study (Alkandari 2002) we had conducted for a 1D gas-oil system.

The transfer functions of this paper are specifically for the sugar-cube idealization of a matrix block, which can be extended to simulation of a match-stick idealization in reservoir modeling. The basic data required are: matrix capillary-pressure curves, densities of the flowing fluids, and matrix block dimensions.

Introduction

Naturally fractured reservoirs contain a significant amount of the known petroleum hydrocarbons worldwide and, hence, are an important source of energy fuels. However, the oil recovery from these reservoirs has been rather low. For example, the Circle Ridge Field in Wind River Reservation, Wyoming, has been producing for 50 years, but the oil recovery is less than 15% (Golder Associates 2004). This low level of oil recovery points to the need for accurate reservoir characterization, realistic geological modeling, and accurate flow simulation of naturally fractured reservoirs to determine the locations of bypassed oil.

Reservoir simulation is the most practical method of studying flow problems in porous media when dealing with heterogeneity and the simultaneous flow of different fluids. In modeling fractured systems, a dual-porosity or dual-permeability concept typically is used to idealize the reservoir on the global scale. In the dual-porosity concept, fluids transfer between the matrix and fractures in the grid-cells while flowing through the fracture network to the wellbore. Furthermore, the bulk of the fluids are stored in the matrix. On the other hand, in the dual-permeability concept, fluids flow through the fracture network and between matrix blocks.

In both the dual-porosity and dual-permeability formulations, the fractures and matrices are linked by transfer functions. The transfer functions account for fluid exchanges between both media. To understand the details of this fluid exchange, an elaborate method is used in this study to model flow in a single matrix block with fractures as boundaries. Our goal is to develop a technique to produce accurate results for use in large-scale modeling work.

This paper (SPE 104580) was accepted for presentation at the SPE Middle East Oil and Gas Show and Conference, Bahrain, 11–14 March 2007, and revised for publication. Original manuscript received for review 11 December 2006. Revised manuscript received for review 14 November 2008. Paper peer approved 27 November 2008.

Motivation

The motivation for this research is two-fold: The first is computational accuracy and the second is speed of computation. As for accuracy, employing fine-grid simulation, proper physics of flow, and an adaptive explicit/implicit formulation should create accurate accounting of flow between the matrix and fracture. As for speed, in spite of the improvements in reservoir characterization and computer speed, it is still necessary to upscale from geocellular models to perform flow simulations. While fine-grid simulation provides the most accurate results, there are usually several million matrix blocks in the geological reservoir model, depending on the size of the reservoir. It is therefore impractical to attempt to model the reservoir by fine-gridding individual matrix blocks.

The transfer-function approach provides the practical solution because data requirement is substantially less and the speed of computation is much greater. However, to have a credible replacement for fine-gridding of individual matrix blocks, the transfer-function approach must produce results nearly as accurately as the fine-grid simulation, which is the main goal of this research.

Literature Review

The heart of the dual-porosity model is the transfer function, which accounts for the transfer of fluids between the fracture and the matrix. The matrix blocks are modeled as sources of fluid exchange within the fracture network (Kazemi and Gilman 1988).

The rudiments of the current models were established by Barenblatt et al. (1960) and Warren and Root (1963). These authors dealt only with single-phase flow in dual-porosity systems and described the transfer function, τ, as:

$$\tau = \sigma \frac{k}{\mu}(p_f - p_m), \qquad (1)$$

where, σ is shape factor, k is matrix permeability, μ is fluid viscosity, and (p_f - p_m) is pressure difference between the fracture and matrix. Warren and Root provided an analytical solution for radial flow for well testing purposes and idealized a fractured reservoir as a set of stacked sugar cubes. Kazemi et al. (1976) extended the Warren and Root (1963) model to multiphase flow and developed a numerical algorithm to solve the fracture-flow equations while accounting for matrix/fracture-fluid transfer through use of a multiphase transfer function.

Hydrocarbon reservoirs produce fluids under a combination of mechanisms that include capillarity, gravity drainage, viscous displacement, pore compaction, and fluid expansion. Depending on the flowing phases present, capillary and gravity forces are generally dominant in fractured reservoirs. These forces can work in tandem or oppose each other (Gilman 2003).

Yamamoto et al. (1971) used a compositional model while Sonier et al. (1988) and Litvak (1985) provided a dynamic model to account for the interaction of gravity and capillary forces in the matrix/fracture system. Gilman (1986) also attempted to better account for gravity forces by solving the finite-difference

equations through use of the water- and oil-flow potential differences between fracture and matrix.

Dual-porosity simulators do not generally account for viscous displacement in the matrix resulting from the flow-potential gradient in the surrounding fractures. Kazemi and Gilman (1988) presented a formulation to properly account for this effect.

Typically, in water-wet systems, part of the production is attributed to capillary-pressure forces, while in tall matrix columns, gravity is the main contributor to production. This has been verified by laboratory experiments (Kyte 1970). Fung (1991) and Uleberg and Kleppe (1996) shed light on gravity drainage and fluid re-infiltration issues.

Capillary-pressure effects on flow in the fracture network have been extensively discussed in literature, but are still not well understood. Mattax and Kyte (1962), Kyte (1970), and Horie et al. (1990) conducted laboratory experiments to elucidate this issue. Also, if one assumes that there is some capillary continuity between matrix blocks across the fractures, then the dual-permeability model can be used as opposed to the dual-porosity model (Fung 1991).

Several authors have addressed the practical aspects of fractured reservoirs (Saidi 1983; Kazemi et al. 1993; Liu et al. 2006; Blair 1964; and Iffly et al. 1972).

Shape Factor

There has been much discussion in the literature in trying to understand the physical and functional form of the shape factor. Shape factor is a geometric factor characteristic of the geometry and boundary conditions of the matrix block. An expression for shape factor was presented by Warren and Root (1963) as follows:

$$\sigma = \frac{4n(n+2)}{l^2}, \quad (2)$$

where n is the number of normal sets of fractures and l is the characteristic length of the matrix block given by:

$$l = \begin{cases} L_x, & n=1 \\ 2L_xL_y/\left(L_x+L_y\right), & n=2 \\ 3L_xL_yL_z/\left(L_xL_y+L_yL_z+L_zL_x\right), & n=3 \end{cases} \quad (3)$$

Kazemi et al. (1976) later proposed a shape-factor expression based on standard seven-point finite-difference as shown below:

$$\sigma = 4\left[\frac{1}{L_x^2}+\frac{1}{L_y^2}+\frac{1}{L_z^2}\right], \quad (4)$$

where L_x, L_y, and L_z represent the dimensions of a matrix block.

Kazemi et al. (1992) and Zhang et al. (1996) used the following shape-factor equation to correlate water imbibition oil-recovery experiments:

$$\sigma = \frac{1}{V}\sum_{j=1}^{J}\frac{A_j}{d_j}, \quad (5)$$

where A_j represents the area for the open surface j of the matrix block, d_j represents the distance from the centre of the matrix block to the open surface j, and V is the volume of the matrix block. This equation was confirmed recently by Heinemann and Mittermeir (2006).

Chang (1993) and Lim and Aziz (1995) have presented the shape factor in various forms. Rangel-German and Kovscek (2003) consider it as a matching parameter that changes with flow regimes and is hence a function of time.

Transfer Function and Gravity Shape Factor

The general approach to modeling matrix fracture-fluid transfer is through a simple transfer function for a single matrix block surrounded by fractures. This transfer function should account for imbibition, gravity drainage, fluid expansion, and molecular diffusion. Then, the transfer function becomes a major building block for dual-porosity/dual-permeability simulation of naturally fractured reservoirs.

To begin with, it can be easily shown that for water-oil flow, the transfer function based on conventional single-porosity formulation (Kazemi et al. 1976) has the following form for the water phase:

$$\tau_w = \sigma\frac{k_m k_{rw}}{\mu}\left\{\left[p_f - p_m\right] - \left(\frac{\sigma_z}{\sigma}\right)\gamma_w\left(D_f - D_m\right)\right\}, \quad (6)$$

and

$$\tau_w = \phi_m\frac{\partial S_{wm}}{\partial t} + \phi_m S_{wm}\left(c_{wm}+c_{\phi m}\right)\frac{\partial p_{wm}}{\partial t}. \quad (7)$$

However, the gravity term in the transfer function is controlled by the height of the matrix block. On the basis of the work of Kazemi and Gillman (1993), accounting for this local effect, Eq. becomes:

$$\tau_w = \sigma\frac{k_m k_{rw}}{\mu}\left\{\left[p_f - p_m\right] + \left(\frac{\sigma_z}{\sigma}\right)\gamma_w\left(h_{wf} - h_{wm}\right)\right\}. \quad (8)$$

The details of the transfer function formulation are presented in the Appendix. Gas diffusion in and out of the matrix block involves interphase mass transfer and phase-equilibrium calculations (Hoteit and Firoozabadi 2006), which will be presented in a future paper.

Finite-Difference Model

Fluid flow in reservoirs is typically modeled numerically with finite-difference discretization of the continuity equation and Darcy law, which results in the pressure equation. For numerical accuracy, we used a fine-grid, 3D implicit pressure explicit saturation (IMPES) formulation, which accounted for gravity, viscous, and capillary forces. Thus, convective flow was the mechanism of mass transfer for water and oil. Molecular diffusion was not included in our numerical experiments because the two phases are immiscible and there is no interphase mass transfer. The details of the formulation are given in the Appendix.

Fig. 1 depicts a schematic of a naturally fractured reservoir segment (Beliveau 1989). For numerical modeling, the fracture/matrix reservoir segment in Fig. 1 can be idealized by a model similar to the cartoon shown in **Fig. 2** (Civan and Rasmussen 2002).

Fig. 2 represents the reservoir as a network of matrix blocks of various sizes surrounded by orthogonal fracture sets. In this paper, we study oil-recovery predictions from one of the matrix blocks only. **Fig. 3** presents the water-oil capillary gravity-force balance for a single cell matrix block for which fluid exchange is approximated with a simple transfer function, τ_w, and a detailed fine-grid model of the same matrix block through use of the equations presented in the following section.

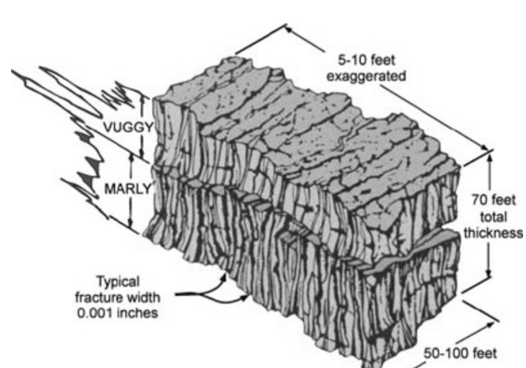

Fig. 1—Schematic of a naturally fractured reservoir segment (after Beliveau 1989).

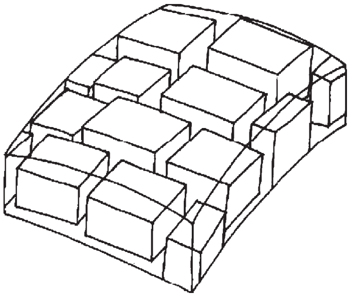

Fig. 2—Idealization of a naturally fractured reservoir (after Civan et al. 2002).

Accounting for Fluid Flow Between the Matrix and Fracture in the Fine-Grid Simulation

The model developed in this study is used to simulate a single matrix block with pressure support at any of its boundaries. Appropriate boundary transmissibilities are used in calculating the transfer of water and oil between the matrix and surrounding fractures, as will be shown later.

Fig. 4a shows the initial oil and water gradients in the matrix and fracture when the matrix block is fully immersed in water. Fig. 4b shows a similar distribution of the fluid gradients for a partially immersed matrix. Furthermore, we assume that the oil expelled from the matrix to the fracture is removed from the fractures surrounding the matrix block.

The matrix block is assumed initially to be above the transition zone and, hence, the water saturation in the matrix block is at the irreducible level. Capillary pressure in the fracture is set equal to zero because of the high fracture permeability. The pressure is specified at the datum, which is a horizontal plane just above the top of the matrix block. The datum pressure and specified fluid gradients are used to calculate phase pressures at any other point in the matrix block. The flow-potential gradient in the horizontal plane in the matrix block is zero; that is,

$$\frac{dp}{dx} = \frac{dp}{dy} = 0. \quad (9)$$

On the other hand,

$$\frac{dp}{dz} = \gamma_o, \quad (10)$$

thus,

$$\int_{p_1}^{p_2} dp = \int_{p_1}^{p_2} \gamma_o dz. \quad (11)$$

This yields:

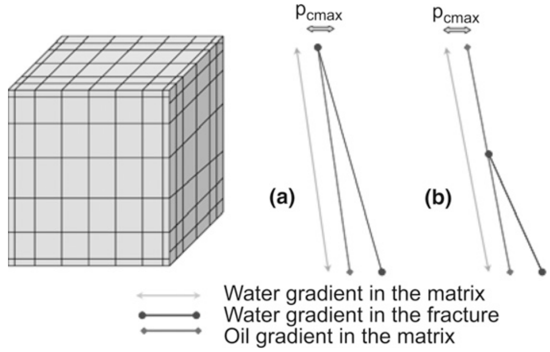

Fig. 4—Initializing a matrix-fracture space: (a) Water-filled fracture, (b) partially water-filled fracture.

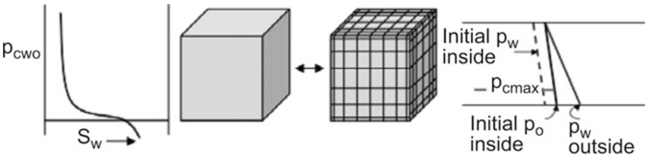

Fig. 3—Schematic of water-oil capillary-gravity force balance for a matrix block.

$$p_2 = p_1 + \gamma_o(z_2 - z_1). \quad (12)$$

The water pressure in the matrix block at any point is calculated by use of the oil pressure and the specified capillary pressure at that point with Eq. 13:

$$p_w^{n+1} = p_o^{n+1} - p_{cwo}^n. \quad (13)$$

The force that drives water from the fracture into the matrix is the difference between the water pressure outside and inside of the matrix block (see Fig. 4). Inside the matrix block, the water phase is initially immobile; thus, its pressure is less than the mobile oil-phase pressure by the capillary pressure at the irreducible water saturation. In time, the capillary force is reduced as water saturation increases in the matrix block, thus shifting the water pressure closer to the oil pressure.

If the system is of mixed wettability, the gravity and capillary forces oppose each other when the water saturation becomes larger than the forced imbibition portion of the capillary pressure curve; thereby, halting the rate of oil expulsion unless water gravity head prevails.

In the fracture, a fixed value of water and/or oil pressure is specified at the matrix top to initialize the entire system.

Transfer-Function Coefficient. Most of the transfer functions in the literature were derived on the basis of the premise that a matrix block is totally surrounded by water at its boundaries (Rangel-German and Kovscek 2003). This is certainly not the case as the fluids surrounding a matrix block move over time to various heights through the fracture network. We have modified the transfer function to account for this reality by assuming that the water-exposed surface in the fracture is proportional to (S_{wf} - S_{wrf}).

Analysis of Results

Various hypothetical water-oil displacement scenarios were carried out to compare the transfer function to the fine-grid model. The models covered a variety of situations by altering the matrix size, wettability, capillary pressure, and the boundary conditions (i.e., the height of the water-oil interfaces in the fractures). The results and explanations for several scenarios are given below.

TABLE 1—MATRIX BLOCK AND GRID DATA USED IN CASE 1

Matrix block dimensions (ft×ft×ft)	50×50×20
Porosity (fraction)	0.20
Matrix permeability (md)	3.20
Maximum capillary pressure (psi)	2.84
Oil viscosity (cp)	2.00
Water viscosity (cp)	1.00
Oil density (lb/ft^3)	50.00
Water density (lb/ft^3)	62.40
Number of grids for each direction	7×7×7
Matrix wettability	Water-wet
S_{orw} (fraction)	0.20
$S_{wi} = S_{wr}$ (fraction)	0.25

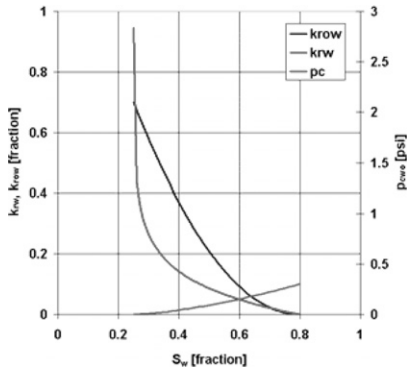

Fig. 5—Relative permeability and capillary pressure used in simulation.

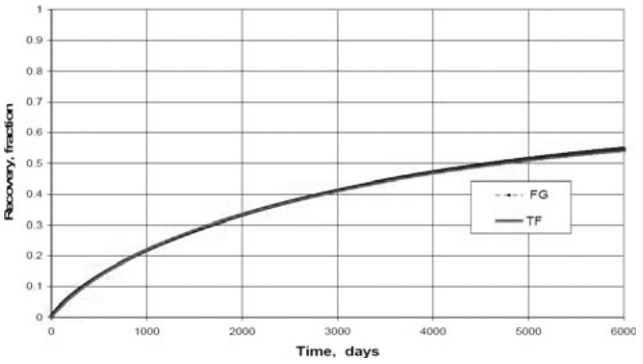

Fig. 6—Matrix oil recovery as a function of time for Case 1.

Case 1—Capillary-Gravity-Dominated Scenario. Table 1 shows the rock and fluid properties of the matrix block for Case 1. **Fig. 5** shows the relative permeability and capillary pressure used in modeling flow for this scenario. **Fig. 6** contains the oil recovery obtained from our new transfer function and the fine-grid model. It can be observed that there is great agreement between both models.

Case 2—Capillary-Dominated Scenario. The intent of this run was to evaluate the response of a matrix block to imbibing fluids when the dominant mechanism of oil production is capillary force. This is usually the case when the matrix blocks are water-wet and small in size. Two runs (Cases 2A and 2B) are presented here and differ only by the size of the matrix block. **Table 2** contains rock, fluid and grid data input for Cases 2A and 2B. Case 2A considers a 50-ft x 50-ft x 1-ft block and Case 2B considers a 20-ft x 20-ft x 5-ft block. **Fig. 7** shows the capillary pressure and relative permeability curves used in modeling flow for Cases 2A and 2B. **Figs. 8 and 9** show a comparison of the oil recovery obtained from both the fine-grid and transfer-function models, for Cases 2A and 2B, respectively. The agreement between the fine-grid and transfer-function model is excellent for both cases in Figs. 8 and 9.

Case 3—Gravity-Dominated Scenario. The purpose of this scenario was to observe the oil-recovery response of a matrix block when the dominant mechanism of production is gravitational

TABLE 2—MATRIX BLOCK AND GRID DATA USED IN CASES 2A and 2B

Matrix block dimensions for Case 2A (ft×ft×ft)	50×50×10
Matrix block dimensions for Case 2B (ft×ft×ft)	20×20×5
Porosity (fraction)	0.20
Matrix permeability (md)	3.20
Maximum capillary pressure (psi)	0.95
Oil viscosity (cp)	2.00
Water viscosity (cp)	1.00
Oil density (lb/ft^3)	50.00
Water density (lb/ft^3)	62.40
Number of grids for each direction	7×7×7
Matrix wettability	Water-wet
S_{orw} (fraction)	0.20
$S_{wi} = S_{wr}$ (fraction)	0.25

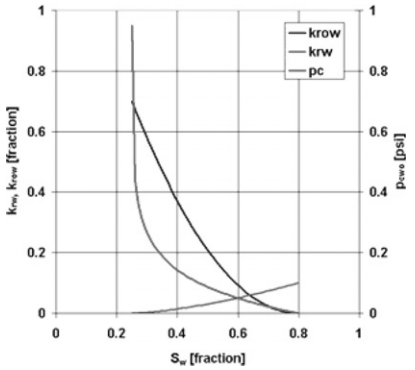

Fig. 7—Relative permeability and capillary pressure used in Cases 2A and 2B.

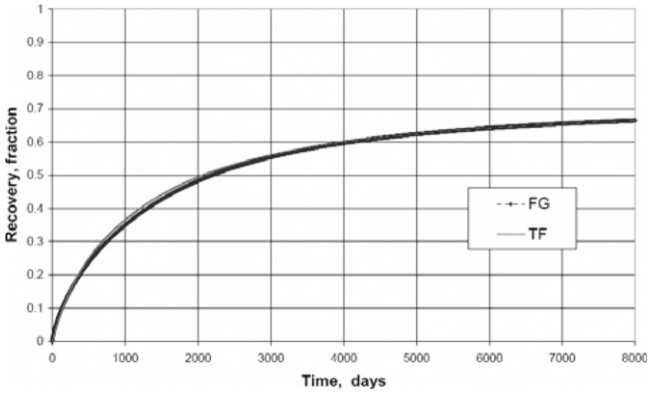

Fig. 8—Matrix oil recovery as a function of time for Case 2A.

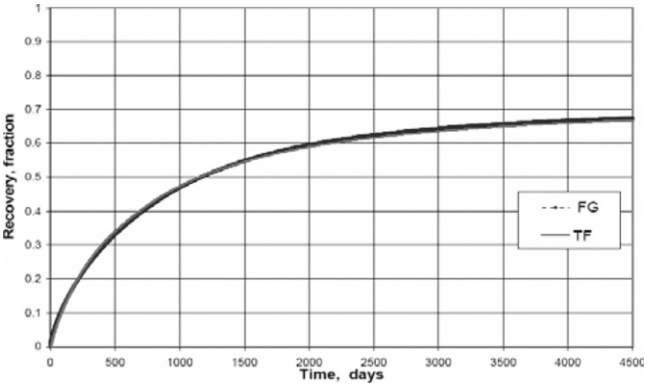

Fig. 9—Oil recovery as a function of time for Case 2B.

TABLE 3—MATRIX BLOCK AND GRID DATA USED IN CASE 3A	
Matrix block dimensions (ft×ft×ft)	20×20×20
Porosity (fraction)	0.20
Matrix permeability (md)	3.20
Maximum capillary pressure (psi)	2.17
Oil viscosity (cp)	2.00
Water viscosity (cp)	1.00
Oil density (lb/ft^3)	50.00
Water density (lb/ft^3)	62.40
Number of grids for each direction	7×7×7
Matrix wettability	Mixed-wet
S_{orw} (fraction)	0.20
$S_{wi} = S_{wr}$ (fraction)	0.25

TABLE 4—MATRIX BLOCK AND GRID DATA USED IN CASE 3B	
Matrix block dimensions (ft×ft×ft)	20×20×5
Porosity (fraction)	0.20
Matrix permeability (md)	3.20
Maximum capillary pressure (psi)	0.87
Oil viscosity (cp)	2.00
Water viscosity (cp)	1.00
Oil density (lb/ft^3)	50.00
Water density (lb/ft^3)	62.40
Number of grids for each direction	7×7×7
Matrix wettability	Mixed-wet
S_{orw} (fraction)	0.20
$S_{wi} = S_{wr}$ (fraction)	0.25

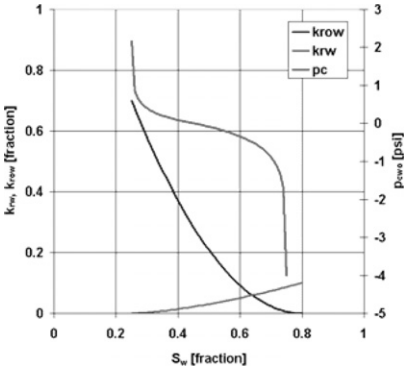

Fig. 10—Relative permeability and capillary pressure used in Case 3A.

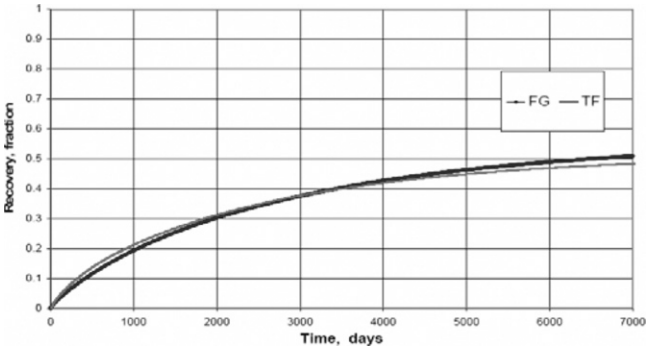

Fig. 11—Matrix oil recovery as a function of time for Case 3A.

force. This is usually the case when the matrix column is long and has mixed wettability. Cases 3A and 3B are presented here and differ by the size of the matrix block and capillary pressure. **Tables 3 and 4** show rock and fluid data used in Cases 3A and 3B, respectively.

Fig. 10 shows the capillary-pressure and relative-permeability curves, representative of a mixed-wet system, used in modeling flow for Case 3A. A comparison of the oil recovery obtained from both the fine-grid model and the transfer function is shown in **Fig. 11.** The counterparts of Figs. 10 and 11 for Case 3B are **Figs. 12 and 13.** The oil-recovery curves in Figs. 11 and 13 show very good agreement between the results from the fine-grid model and the transfer-function approach. However, it should be noted that the match is not nearly as excellent as those presented in the capillary-dominated cases or when both capillary and gravity forces contribute significantly to production. One reason for this difference would be the nature of the mixed-wettability capillary-pressure region.

Case 4—Effect of Partially Water-Filled Fractures on Recovery. Up to this point, we have modeled the performance of a single matrix block surrounded by water in the fracture. Now, we examine the effect of the partially water-filled fracture on production from a matrix block.

Two cases are presented (Cases 4A and 4B), which differ by the magnitude of the capillary pressure (with the maximum of

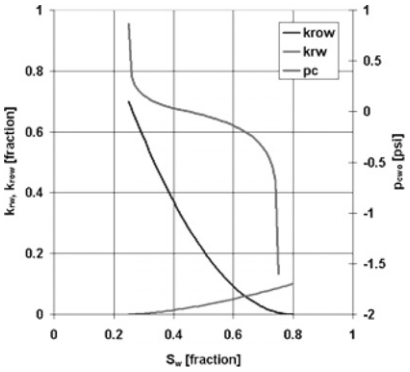

Fig. 12—Relative permeability and capillary pressure used in Case 3B.

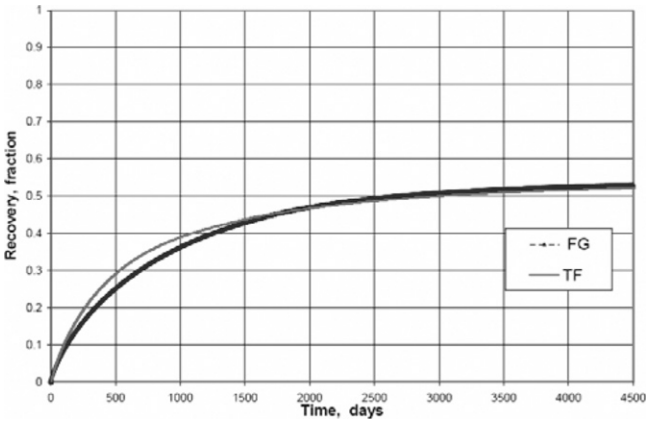

Fig. 13—Matrix oil recovery as a function of time for Case 3B.

TABLE 5—MATRIX BLOCK AND GRID DATA USED IN CASES 4A and 4B	
Matrix block dimensions (ft×ft×ft)	20×20×20
Porosity (fraction)	0.20
Matrix permeability (md)	3.20
Maximum capillary pressure for Case 4A (psi)	2.17
Maximum capillary pressure for Case 4B (psi)	0.95
Oil viscosity (cp)	2.00
Water viscosity (cp)	1.00
Oil density (lb/ft^3)	50.00
Water density (lb/ft^3)	62.40
Number of grids for each direction	3×3×7
Matrix wettability for Case 4A	Mixed-wet
Matrix wettability for Case 4B	Water-wet
S_{orw} (fraction)	0.20
$S_{wi} = S_{wr}$ (fraction)	0.25

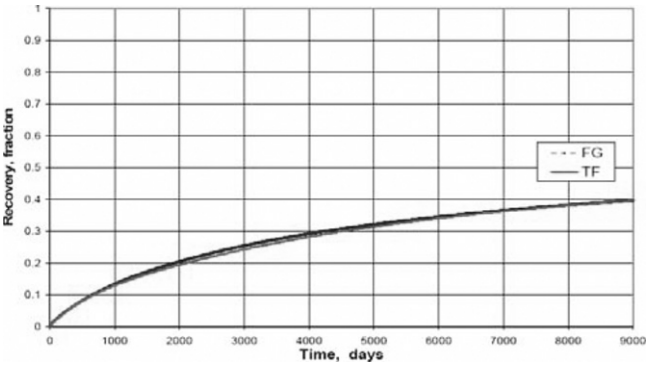

Fig. 15—Matrix oil recovery as a function of time for Case 4A.

2.17 psi for Case 4A and 0.95 for Case 4B). For both cases, it was assumed that the fractures around the matrix block contained 50% water and 50% oil. **Table 5** presents the rock and fluid properties used for Cases 4A and 4B.

Fig. 14 shows the relative-permeability and capillary-pressure curves used in modeling the fluid flow in Case 4A. The comparison of the oil recovery from the matrix block through use of both the modified transfer function and the fine-grid model is shown in **Fig. 15.** Similarly, the relative-permeability and capillary-pressure curves used in Case 4B and the comparison of the oil recovery from the matrix block through use of both the modified transfer

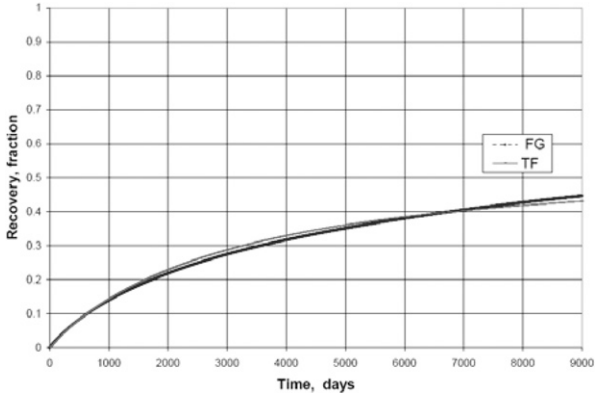

Fig. 17—Matrix oil recovery as a function of time for Case 4B.

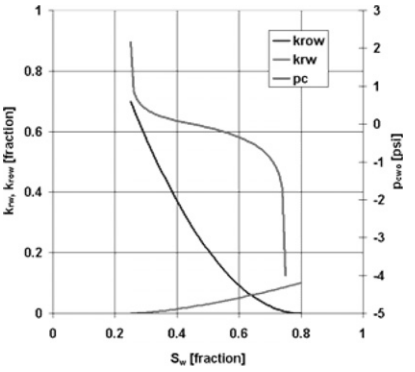

Fig. 14—Relative permeability and capillary pressure used in Cases 4A.

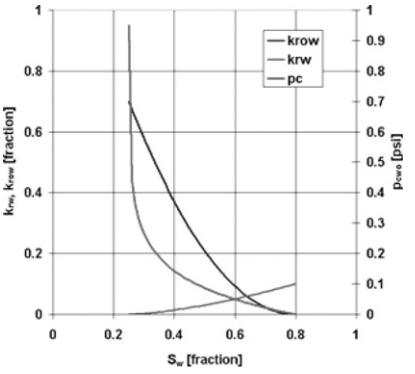

Fig. 16—Relative permeability and capillary pressure used in Case 4B.

function and the fine-grid model are shown in **Figs. 16 and 17,** respectively. Figs. 15 and 17 show an excellent match between the fine-grid and the transfer-function simulation results.

Case 5—Old and New Transfer-Function Comparison. In this scenario, we present a simulation run comparing the oil recovery of the unmodified and modified transfer functions to the fine-grid model to show the improvements to the old transfer function. **Table 6** shows the properties of the matrix block for Case 5, and **Fig. 18** contains the relative-permeability and capillary-pressure plots. **Fig. 19** shows the comparison of the oil recovery between

TABLE 6—MATRIX BLOCK AND GRID DATA USED IN CASE 5	
Matrix block dimensions (ft×ft×ft)	20×20×20
Porosity (fraction)	0.20
Matrix permeability (md)	3.20
Maximum capillary pressure (psi)	0.95
Oil viscosity (cp)	2.00
Water viscosity (cp)	1.00
Oil density (lb/ft^3)	50.00
Water density (lb/ft^3)	62.40
Number of grids for each direction	7×7×7
Matrix wettability	Water-wet
S_{orw} (fraction)	0.20
$S_{wi} = S_{wr}$ (fraction)	0.25

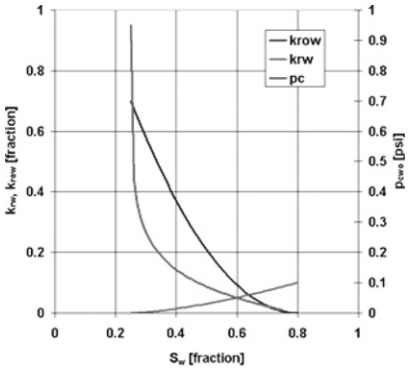

Fig. 18—Relative permeability and capillary pressure used in Case 5.

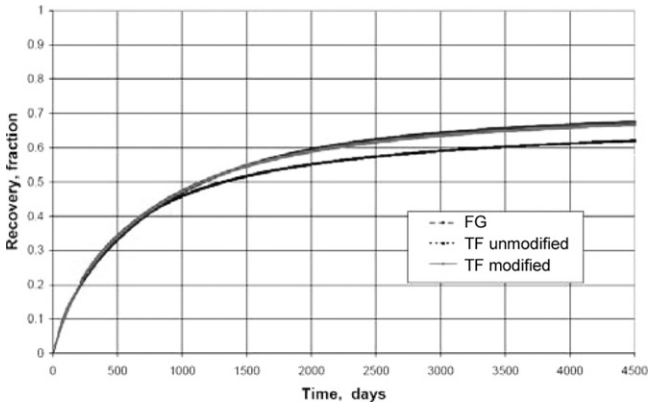

Fig. 19—Matrix oil recovery as a function of time for Case 5.

the transfer functions and the fine-grid model. It is immediately obvious from the recovery plot that without the modification to the old transfer function (Moreno et al. 2004) a match with the fine-grid model cannot be obtained.

Case 6—Buckley-Leverett Waterflood by Use of the Old and New Transfer Function. In Case 5, the old and new transfer functions were used to compare oil recovery from a single matrix block model. Here, we compare the oil recovery in a one-dimensional Buckley-Leverett waterflood model in a naturally fractured reservoir through use of the same transfer functions. Each grid cell could contain several matrix blocks. **Table 7** provides the rock, fluid, and grid data for this scenario. The equations used for the waterflood in differential and finite difference forms are

$$-u_{tf}\frac{\partial f_{wf}}{\partial x}-\frac{\tau_w}{\phi_f}=\frac{\partial S_{wf}}{\partial t}, \quad \ldots\ldots\ldots\ldots\ldots\ldots\ldots\ldots (14)$$

and

$$-u_{tf}\frac{f^n_{wf_i}-f^n_{wf_{i-1}}}{\Delta x_i}-\frac{\tau^n_{w_i}}{\phi_f}=\frac{S^{n+1}_{wf_i}-S^n_{wf_i}}{\Delta t}, \quad \ldots\ldots\ldots\ldots\ldots (15)$$

where

$$u_{tf}=\frac{q_{tf}}{\Delta y\Delta z\phi_f}. \quad \ldots\ldots\ldots\ldots\ldots\ldots\ldots\ldots\ldots\ldots\ldots (16)$$

TABLE 7—MATRIX BLOCK AND GRID DATA USED IN CASE 6

Matrix block dimensions (ft×ft×ft)	5×5×5
Matrix porosity (fraction)	0.20
Fracture porosity (fraction)	0.001
Number of grids for each direction	50×10×5
Distance between injector and producer (ft)	1500.00
Water viscosity (cp)	1.00
Oil viscosity (cp)	2.00
Water density (lb/ft^3)	62.40
Oil density (lb/ft^3)	50.00
Total rate, q_{tf} (ft^3/day)	3.75
S_{wif} / S_{orf} / S_{wrf} (fraction)	0.00
Matrix permeability (md)	3.20
Maximum capillary pressure (psi)	0.50
S_{orw} (fraction)	0.20
S_{wi} = S_{wr} (fraction)	0.25

Fig. 20 compares both the oil-production rate and oil-recovery obtained from the Buckley-Leverett waterflood by use of both the old and new transfer functions.

Conclusions

The objective of this work was to improve modeling of matrix/fracture-fluid transfer through use of a transfer function by comparing to the output of a fine-grid matrix-block simulation. Below is the summary of the results of this research.

1. An accurate transfer function has been developed to account for matrix/fracture-fluid transfer in dual-porosity models. The approach can be extended to dual-permeability models as well. The transfer-function approach is more practical and much faster than fine-gridding each matrix block. In fact, fine gridding of every individual matrix block is truly impossible because of the high degree of reservoir heterogeneity.
2. A simple modification was made to an earlier fracture-matrix transfer function to more accurately account for the gravity force.
3. We have also presented the formulation of water-soluble surfactant for improved waterflooding. Specifically, we have shown how the diffusion term appears in the transfer function.
4. Finally, in this paper we have shown a clear relationship between capillarity, gravity, fluid compressibility (expansibility), and molecular diffusion when applicable.

Nomenclature

A = cross sectional area normal to flow, ft^2
A_j = area of an open surface of a matrix block, ft^2
c_t = total compressibility, psi^{-1}
c_ϕ = rock compressibility, psi^{-1}
$\vec{C}_w$ = capillary force flow velocity vector, ft/day

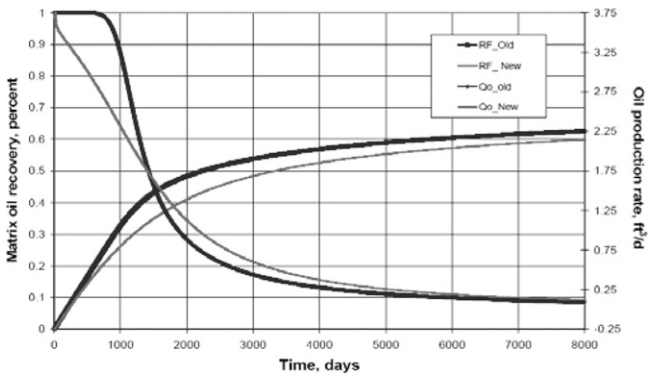

Fig. 20—Oil production rate and matrix oil recovery as a function of time for Case 6.

d = distance from the centre of a matrix block to an open bounding surface, ft
D = depth, ft
f_w = fractional flow, fraction
$\vec{G}_w$ = gravity force flow velocity vector, ft/day
h = gravity head, ft
j = open surface
k = 0.006328 x absolute permeability, md
k_r = relative permeability
k_r^* = relative permeability endpoint
k_{ro}^* = maximum relative permeability to oil
$\overline{\overline{k}}_f$ = 0.006328 × fracture permeability tensor, md
k_{rw}^* = maximum relative permeability to water
l = matrix block characteristic length, ft
L = matrix block dimension, ft
n = number of fracture sets
n_o = oil exponent
n_w = water exponent
p = phase pressure, psi
p_f = fracture pressure, psi
p_m = matrix pressure, psi
q_{tf} = total fracture reservoir flow rate, ft^3 /day
$\hat{q}_{tf}$ = total fracture reservoir flow rate, ft^3/ft^3/day
S = saturation, fraction
S_{wr} = irreducible water saturation
S_{orw} = residual oil saturation
t = time, day
T_o = oil-boundary transmissibility
T_w = water boundary transmissibility
$\vec{u}$ = interstitial velocity vector, ft/day
$\vec{v}$ = Darcy velocity vector, ft/day
V = volume of a matrix block, ft^3
VR = volume of a gridblock, ft^3
γ = fluid gravity gradient, psi/ft
Δx = x-direction grid dimension, ft
Δy = y-direction grid dimension, ft
Δz = z-direction grid dimension, ft
λ = mobility coefficient, cp^{-1}
μ = viscosity, cp
ρ = density, lbm/ft^3
σ = matrix block shape factor, $1/ft^2$
τ = matrix-fracture transfer function, 1/day
ϕ = porosity, fraction
τ_w = transfer function
∇ = gradient operator
$\nabla \cdot$ = divergence operator

Subscripts

f = fracture
m = matrix
o = oil
w = water

Acknowledgments

This research was conducted at the Marathon Center of Excellence for Reservoir Studies at Colorado School of Mines. We acknowledge the funding by Marathon Oil Co., Abu Dhabi Nat'l Oil Co., Saudi Aramco, and Repsol-YPF.

References

Al-Kandari, H.A., Kazemi, H., and Van Kirk, C.W. 2002. Gas Injection Enhanced Oil Recovery in High Relief Naturally Fractured Reservoirs. Presented at the 2002 Kuwait International Petroleum Conference and Exhibition, Kuwait City, State of Kuwait, November.

Barenblatt, G.I., Zheltov, Iu.P., and Kochina, I.N. 1960. Basic concepts in the theory of seepage of homogeneous liquids in fissured rocks. *Journal of Applied Mathematics and Mechanics* **24** (5): 1286–1303. DOI:10.1016/0021-8928(60)90107-6.

Beliveau, D. 1989. Pressure Transients Characterize Fractured Midale Unit. *JPT* **41** (12): 1354–1362; *Trans.,* AIME, **287**. SPE-15635-PA. DOI: 10.2118/15635-PA.

Blair, P.M. 1964. Calculation of Oil Displacement by Countercurrent Water Imbibition. *SPEJ* **4** (3): 195-202; *Trans.,* AIME, **231**. SPE-873-PA. DOI: 10.2118/873-PA.

Chang, M-M. 1993. NIPER-696: Deriving the shape factor of a fractured rock matrix. Technical report, Contract No. DE93000170, US DOE, Washington, DC (September 1993). DOI: 10.2172/10192737.

Civan, F. and Rasmussen, M.L. 2002. Analytical Hindered-Matrix-Fracture Transfer Models for Naturally Fractured Petroleum Reservoirs. Paper SPE 74364 presented at the SPE International Petroleum Conference and Exhibition in Mexico, Villahermosa, Mexico, 10–12 February. DOI: 10.2118/74364-MS.

Fung, L.S.K. 1991. Simulation of Block-to-Block Processes in Naturally Fractured Reservoirs. *SPERE* **6** (4): 477–484. SPE-20019-PA. DOI: 10.2118/20019-PA.

Gilman, J.R. 1986. An Efficient Finite-Difference Method for Simulating Phase Segregation in the Matrix Blocks in Double-Porosity Reservoirs. *SPERE* 1 (4): 403–413; *Trans.,* AIME, **281**. SPE-12271-PA. DOI: 10.2118/12271-PA.

Gilman, J.R. 2003. Practical aspects of simulation of fractured reservoirs. Presented at the International Forum on Reservoir Simulation, Buhl, Baden-Baden, Germany, 23–27 June.

Gilman, J.R. and Kazemi, H. 1988. Improved Calculations for Viscous and Gravity Displacement in Matrix Blocks in Dual-Porosity Simulators. *JPT* **40** (1): 60–70; *Trans.,* AIME, **285**. SPE-16010-PA. DOI: 10.2118/16010-PA.

Heinemann, Z.E. and Mittermeir, M.G. 2006. Rigorous derivation of the Kazemi-Gilman-Elsharkawy generalized dual-porosity shape factor. Paper B044 presented at the 10th European Conference on the Mathematics of Oil Recovery, Amsterdam, 4–7 September.

Horie, T., Firoozabadi, A., and Ishimoto, K. 1990. Laboratory Studies of Capillary Interaction in Fracture/Matrix Systems. *SPERE* **5** (3): 353–360. SPE-18282-PA. DOI: 10.2118/18282-PA.

Hoteit, H. and Firoozabadi, A. 2006. Numerical Modeling of Diffusion in Fractured Media for Gas Injection and Recycling Schemes. Paper SPE 103292 presented at the SPE Annual Technical Conference and Exhibition, San Antonio, Texas, USA, 24–27 September. DOI: 10.2118/103292-MS.

Iffly, R., Rousselet, D.C., and Vermeulen, J. L. 1972. Fundamental Study of Imbibition in Fissured Oil Fields. Paper SPE 4102 presented at the Fall Meeting of the Society of Petroleum Engineers of AIME, San Antonio, Texas, USA, 8–11 October. DOI: 10.2118/4102-MS.

Kazemi, H. and Gilman, J.R. 1993. Multiphase flow in fractured petroleum reservoirs. In *Flow and Contaminant Transport in Fractured Rock*, ed. J. Bear, C.-F. Tsang, G. de Marsily, 267–323. San Diego, California: Academic Press.

Kazemi, H., Merrill, J.R, Porterfield, K.L., and Zeman, P.R. 1976. Numerical Simulation of Water-Oil Flow in Naturally Fractured Reservoirs. *SPEJ* **16** (6): 317–326; *Trans.,* AIME, **261**. SPE-5719-PA. DOI: 10.2118/5719-PA.

Kleppe, J. and Morse, R.A. 1974. Oil Production From Fractured Reservoirs by Water Displacement. Paper SPE 5084 presented at the Fall Meeting of the Society of Petroleum Engineers of AIME, Houston, 6–9 October. DOI: 10.2118/5084-MS.

Kyte, J.R. 1970. A Centrifuge Method To Predict Matrix-Block Recovery in Fractured Reservoirs. *SPEJ* **10** (2): 161–170; *Trans.,* AIME, **249**. SPE-2729-PA. DOI: 10.2118/2729-PA.

Lim, K.T. and Aziz, K. 1995. Matrix-fracture transfer functions for dual porosity simulators. *J. Pet. Sci. Eng.* **13** (3–4): 169–178. DOI: 10.1016/0920-4105(95)00010-F.

Litvak, B.L. 1985. Simulation and characterization of naturally fractured reservoirs. *Proc.,* Reservoir Characterization Technical Conference, Dallas, 561–583.

Lu, H., Di Donato, G., and Blunt, M.J. 2006. General Transfer Functions for Multi-Phase Flow. Paper SPE 102542 presented at the SPE Annual

Technical Conference and Exhibition, San Antonio, Texas, USA, 24–27 September. DOI: 10.2118/102542-MS.

Mattax, C.C. and Kyte, J.R. 1962. Imbibition Oil Recovery From Fractured, Water-Drive Reservoir. *SPEJ* **2** (2): 177–184; *Trans.,* AIME, **225**. SPE-187-PA. DOI: 10.2118/187-PA.

Moreno, J., Kazemi, H., and Gilman, J.R. 2004. Streamline Simulation of Countercurrent Water-Oil and Gas-Oil Flow in Naturally Fractured Dual-Porosity Reservoirs. Paper SPE 89880 presented at the SPE Annual Technical Conference and Exhibition, Houston, 26–29 September. DOI: 10.2118/89880-MS.

Rangel-German, E.R. and Kovscek, A.R. 2003. Time-Dependent Matrix-Fracture Shape Factors for Partially and Completely Immersed Fractures. Paper SPE 84411 presented at the SPE Annual Technical Conference and Exhibition, Denver, 5–8 October. DOI: 10.2118/84411-MS.

Saidi, A.M. 1983. Simulation of Naturally Fractured Reservoirs. Paper SPE 12270 presented at the SPE Reservoir Simulation Symposium, San Francisco, 15–18 November. DOI: 10.2118/12270-MS.

Sonier, F., Souillard, P, and Blaskovich, F.T. 1988. Numerical Simulation of Naturally Fractured Reservoirs. *SPERE* **3** (4): 1114–1122; *Trans.,* AIME, **285**. SPE-15627-PA. DOI: 10.2118/15627-PA.

Uleberg, K. and Kleppe, J. 1996. Dual porosity, dual permeability formulation for fractured reservoir simulation. Presented at the Norwegian University of Science and Technology (NTNU), Trondheim RUTH Seminar, Stavanger.

Warren, J.E. and Root, P.J. 1963. The Behavior of Naturally Fractured Reservoirs. SPEJ 3 (3): 245–255; Trans., AIME, 228. SPE-426-PA. DOI: 10.2118/426-PA.

Yamamoto, R.H., Padgett, J.B., Ford, W.T., and Boubeguira, A. 1971. Compositional Reservoir Simulation for Fissured Systems—The Single-Block Model. *SPEJ* **11** (2): 113–128. SPE-2666-PA. DOI: 10.2118/2666-PA.

Zhang, X., Morrow, N.R., and Ma, S. 1996. Experimental Verification of a Modified Scaling Group for Spontaneous Imbibition. SPERE 11 (4): 280–285. SPE-30762-PA. DOI: 10.2118/30762-PA.

Appendix—Pressure and Velocity Equations

The global pressure equation in compact notation has the following form (Moreno et al. 2004):

$$\nabla \cdot \left[\left(\overline{\overline{k}} \lambda_t \right) \nabla p_o - \vec{G} - \vec{C} \right] + \hat{q}_t = \phi c_t \frac{\partial p_o}{\partial t}, \quad \text{(A-1)}$$

where

$$\vec{G} = (\lambda_w \gamma_w + \lambda_o \gamma_o) \overline{\overline{k}} \nabla D, \quad \text{(A-2)}$$

$$\vec{C} = \lambda_w \overline{\overline{k}} \nabla p_{cwo}, \quad \text{(A-3)}$$

and

$$\hat{q}_t = q_t / (\Delta x \Delta y \Delta z). \quad \text{(A-4)}$$

After solving the pressure equation, the following equation can be used to calculate the total velocity of flowing phases:

$$\vec{v}_t = \vec{v}_o + \vec{v}_w = -\overline{\overline{k}} [\lambda_t \nabla p_o - (\lambda_w \gamma_w + \lambda_o \gamma_o) \nabla D - \lambda_w \nabla p_{cwo}]. \quad \text{(A-5)}$$

The Saturation Equation. The water-saturation equation in a slightly compressible water-oil system is

$$-\left(\nabla \cdot f_w \vec{v}_t + \vec{G}_w - \vec{C}_w \right) = \phi \frac{\partial S_w}{\partial t} + \phi S_w \left(c_w + c_\phi \right) \frac{\partial p_w}{\partial t}. \quad \text{(A-6)}$$

The gravity and capillary terms in Eq. are given, respectively, by

$$\vec{G}_w = f_w \lambda_o \overline{\overline{k}} (\gamma_w - \gamma_o) \nabla D, \quad \text{(A-7)}$$

and

$$\vec{C}_w = f_w \lambda_o \overline{\overline{k}} \nabla p_{cwo}. \quad \text{(A-8)}$$

The fractional flow of water is defined by:

$$f_w = \frac{\lambda_w}{\lambda_t}. \quad \text{(A-9)}$$

Flow-Rate Calculations. Fluid rates in and out of the matrix block (for the fine-grid model) are calculated at all open boundaries by use of the product of the phase Darcy velocities at the boundaries and respective cross sectional areas. For example, the oil and water rates can be calculated, respectively, as follows:

$$q_o = v_o A, \quad \text{(A-10)}$$

and

$$q_w = v_w A. \quad \text{(A-11)}$$

The rates can also be calculated by use of the product of the boundary transmissibilities, phase pressure, and gravity head, as shown in the equations below:

$$q_o = -T_o (\nabla p_o - \gamma_o \nabla D), \quad \text{(A-12)}$$

and

$$q_w = -T_w (\nabla p_w - \gamma_w \nabla D), \quad \text{(A-13)}$$

where T_o and T_w are the oil- and water-boundary transmissibilities between the fracture and matrix given here:

$$T_{ox} = 0.006328\, k_m \lambda_{om} \frac{\Delta y \Delta z}{\Delta x / 2}, \quad \text{(A-14)}$$

and

$$T_{wx} = 0.006328\, k_m \lambda^*_{wm} \frac{\Delta y \Delta z}{\Delta x / 2}. \quad \text{(A-15)}$$

The relative permeability in $\lambda^*_{wm}$is the water-relative permeability endpoint at residual oil saturation in the matrix (core). Oil recovery is then calculated by a simple time integration of the oil-production rate. An equivalent calculation is the ratio of the sum of the oil pore volume in the grid blocks and the total-oil pore volume in the system, which is,

$$RF = \frac{\int_{t_o}^{tn} q_o dt}{OOIP}. \quad \text{(A-16)}$$

Rock and Fluid Properties. The relative permeability to oil and water are given by the following Corey-Brooks relative-permeability equations:

$$k_{rw} = k^*_{rw} \left[\frac{S_w - S_{wr}}{1 - S_{wr} - S_{orw}} \right]^{nw}, \quad \text{(A-17)}$$

and

$$k_{row} = k^*_{row} \left[\frac{1 - S_w - S_{orw}}{1 - S_{wr} - S_{orw}} \right]^{no}. \quad \text{(A-18)}$$

When the fracture is the upstream node, the relative permeability of the fluid entering the matrix is taken to be the maximum relative permeability in the matrix. The same assumption is used in a single cell fracture-matrix transfer function.

For capillary pressure, we used the following equations for water-wet and mixed-wettability matrix, respectively:

$$p_{cwo}(S_w) = \alpha_2 \ln\left[\frac{1 - S_{ox} - S_{wr}}{S_w - S_{wr}}\right]; for\ S_{wr} < S_w < S_{wx}, \quad \text{(A-19)}$$

and

$$p_{cwo}(S_w) = \alpha_1 \ln\left[\frac{1 - S_{wx} - S_{orw}}{1 - S_w - S_{orw}}\right]; for\ S_{wx} < S_w < 1 - S_{orw}, \quad \text{(A-20)}$$

where

$$\alpha_2 = -\alpha_1\left[\frac{S_{wx} - S_{wr}}{1 - S_{wx} - S_{orw}}\right]. \quad \text{(A-21)}$$

In these equations, S_{wx} depends on the degree of wettability. The smaller the value, the more oil-wet the system is and vice-versa. Other rock and fluid properties, such as porosity, viscosity, and formation-volume factor, are assumed to be very mild functions of pressure and, hence, are held invariant.

Dual-Porosity Formulation. The pressure and water saturation equations used in modeling water-oil flow in naturally fractured reservoirs are given below (Kazemi 2004):

$$\nabla\cdot\left[\left(\overline{\overline{k}}_f\lambda_{tf}\right)\nabla p_{of} - \vec{G}_{wf} - \vec{C}_{wf}\right] - (\tau_w + \tau_o) + \hat{q}_{tf} = (\phi c_t)_f\frac{\partial p_{of}}{\partial t} \quad \text{(A-22)}$$

and

$$-\left(\nabla\cdot f_{wf}\vec{v}_{tf} + \vec{G}_{wf} + \vec{C}_{wf}\right) - \tau_w = \phi_f\frac{\partial S_{wf}}{\partial t} + \phi_f S_{wf}\left(c_{wf} + c_{\phi f}\right)\frac{\partial p_{wf}}{\partial t} \quad \text{(A-23)}$$

where

$$\tau_o + \tau_w = \phi_m c_{tm}\frac{\partial p_{om}}{\partial t} - \phi_m S_{wm}\left(c_{wm} + c_{\phi m}\right)\frac{\partial p_{cwom}}{\partial t}, \quad \text{(A-24)}$$

$$\tau_w = \phi_m\frac{\partial S_{wm}}{\partial t} + \phi_m S_{wm}\left(c_{wm} + c_{\phi m}\right)\left(\frac{\partial p_{om}}{\partial t} - \frac{\partial p_{cwom}}{\partial t}\right), \quad \text{(A-25)}$$

and

$$\tau_w = \sigma k_m\left(\frac{\lambda_{wf/m}\lambda_{om/f}}{\lambda_t}\right)\left[\begin{array}{l}\left(p_{cwom} - p_{cwof}\right)\\ +\left(\frac{\sigma_z}{\sigma}\right)(\gamma_w - \gamma_o)\left(h_{wf} - h_{wm}\right)\end{array}\right]. \quad \text{(A-26)}$$

Eq. A-26 can be obtained from Eq. by assuming $\tau_w + \tau_o = 0$, as was similarly done in a previous paper (Moreno et al. 2004), which excluded the term σ_z/σ.

$$\vec{G}_{wf} = f_{wf}\lambda_{of}\overline{\overline{k}}_f(\gamma_w - \gamma_o)\nabla D_f, \quad \text{(A-27)}$$

$$\vec{C}_{wf} = f_{wf}\lambda_{of}\overline{\overline{k}}_f\nabla p_{cwof}, \quad \text{(A-28)}$$

$$\lambda_t = \lambda_{wf/m} + \lambda_{om/f}, \quad \text{(A-29)}$$

$$h_{wf} = \left[\frac{S_{wf} - S_{wrf}}{1 - S_{orwf} - S_{wrf}}\right]L_z, \quad \text{(A-30)}$$

$$h_{wm} = \left[\frac{S_{wm} - S_{wrm}}{1 - S_{orwm} - S_{wrm}}\right]L_z, \quad \text{(A-31)}$$

$$h_{of} = L_z - h_{wf}, \quad \text{(A-32)}$$

$$h_{om} = L_z - h_{wm}, \quad \text{(A-33)}$$

and

$$\sigma_z = \frac{4}{L_z^2}. \quad \text{(A-34)}$$

The implementation of Eq. is very easy in the IMPES formulation because it eliminates the phase pressures. Furthermore, this form clearly shows the interaction between gravity and capillarity. The relative effect of capillary to gravity is shown by the relative magnitude of the capillary term $\left(p_{cwom} - p_{cwof}\right)$vs. the gravity term $\left(\frac{\sigma_z}{\sigma}\right)(\gamma_w - \gamma_o)\left(h_{wf} - h_{wm}\right)$. For instance, if the capillary term is 3 psi (for a water-wet system), and the gravity term is 1 psi, corresponding to a height of 10 ft, then the capillary and gravity add to 4 psi and capillary is much more important than gravity. However, if the capillary term is –3 psi (for an oil-wet system), the combined effect of capillary and gravity is –2 psi, thus water will not enter the matrix. In regards to viscous effects, the examples we have provided for the matrix-fluid transfer, there is no pure viscous displacement and all displacements take place by the interaction of capillary and gravity forces. However, in the field simulator, the viscous effect is accounted for, such as in the work by Kazemi and Gilman (1988). Finally, this form allows the use of the IMPES, instead of a fully implicit formulation for a dual-porosity reservoir. If we include compressibility in the transfer function, Eq. , then the transfer function becomes:

$$\tau_w = \sigma k_m\left\{\begin{array}{l}\left(\frac{\lambda_{wf/m}\lambda_{om/f}}{\lambda_t}\right)\left[\begin{array}{l}\left(p_{cwom} - p_{cwof}\right)\\ +\left(\frac{\sigma_z}{\sigma}\right)(\gamma_w - \gamma_o)\left(h_{wf} - h_{wm}\right)\end{array}\right]\\ +\left(\frac{\lambda_{wf/m}}{\lambda_t}\right)\left[\begin{array}{l}\phi_m c_{tm}\frac{\partial p_{om}}{\partial t}\\ -\phi_m S_{wm}\left(c_{wm} + c_{\phi m}\right)\frac{\partial p_{cwom}}{\partial t}\end{array}\right]\end{array}\right\}. \quad \text{(A-35)}$$

Adetayo Balogun works for Shell E&P. He holds BS and MS degrees in petroleum engineering from the Colorado School of Mines. **Hossein Kazemi** is the Chesebro' Distinguished Professor of Petroleum Engineering at the Colorado School of Mines and Co-director of Marathon Center of Excellence for Reservoir Studies (MCERS). He retired from Marathon Oil Company in 2001 after serving as Research Scientist, Senior Technical Consultant, Director of Production Research, Manager of Reservoir Technology, and Executive Technical Fellow at Marathon Petroleum Technology Center in Littleton, Colorado. At CSM he has taught graduate courses in petroleum engineering and supervised graduate research in reservoir modeling, well testing, and improved oil and gas recovery He holds BS and PhD degrees in petroleum engineering from the University of Texas at Austin. Kazemi is a member of the National Academy of Engineering (NAE), a Distinguished and an Honorary Member of the Society of Petroleum Engineers (SPE). He has published numerous technical papers and has served as Distinguished Author and Speaker for the SPE. **Erdal Ozkan** is a professor of Petroleum Engineering and Co-director of MCERS at the Colorado School of Mines. He has taught at Istanbul Technical University and the Colorado School of Mines. His main research interests are pressure-transient analysis, modeling fluid flow in porous media, horizontal well technology, and unconventional reservoirs. He is the author or co-author of numerous technical papers and a book. He holds BS and MS degrees from Istanbul Technical University and a PhD degree from the University of Tulsa, all in petroleum engineering. He served as the Executive Editor of *SPE Reservoir Evaluation & Engineering Journal* and as the Editor in Chief of Elsevier B.V. *Journal of Petroleum Science and Engineering*. He has

chaired and served as the technical committee member for several SPE forums, workshops, and conferences. Ozkan is the recipient of the 2007 SPE Formation Evaluation Award. **Mohammed Al-Kobaisi** is a Reservoir Engineer with Abu Dhabi National Oil Company (ADNOC). He holds BS and MS degrees in petroleum engineering from the Colorado School of Mines, where he is currently a PhD candidate. **Benjamin Ramirez** is a Reservoir Engineer with Marathon Oil Corporation and a PhD candidate at the Colorado School of Mines. He holds a BS degree in mechanical engineering from Universidad de los Andes and an MS degree in petroleum engineering from the Colorado School of Mines.